Materials International
Open Access Journal (ISSN: 2668-5728)

Article
Volume 6, Issue 2, 2024, 11
https://doi.org/10.33263/Materials62.011

The Mathematical Modeling for the Domoic Acid Galvanostatic Determination in Oyster Products over an Undoped Conducting Polymer

Volodymyr V. Tkach [1,*], Tetiana V. Morozova [2], Marta V. Kushnir [1], Sílvio C. de Oliveira [3], Viktor V. Kryvetskyi [4], Inna I. Kryvetska [4], Igor V. Kryvetskyi [4], Igor G. Biryuk [4], Tetiana B. Sykyrytska [4], Yana G. Ivanushko [4], Alla V. Velyka [4], Petro I. Yagodynets [1,*], Adriano O. da Silva [5], Jarem R. Garcia [6], José Inácio Ferrão da Paiva Martins [7], Gennadii F. Tkach [8], Oleg P. Melnyk [8], Oleksii O. Melnyk [8], Maria V. Melnyk [8], Maria João Monteiro [9], Lilia O. Nikitchenko [10], Iryna G. Patseva [11], Vitalina Lukyanova [11], Liudmyla Mohelnytska [11]

1 Chernivtsi National University, 58001, Kotsyubynsky Str. 2, Chernivtsi, Ukraine
2 National Transport University, 02000, Omelianovych-Pavlenko Str. 1, Kyiv, Ukraine
3 Institute of Chemistry. Federal University of Mato Grosso do Sul, 79074 – 460, Av. Sen. Felinto Müller, 1555, Vila Ipiranga, Campo Grande, MS, Brazil
4 Bukovinian State Medical University, 58001, Teatralna Sq, 9, Chernivtsi, Ukraine
5 Federal University of the West of Pará, Juruti Campus, 68170 – 000, Rua Veríssimo de Souza Andrade, s/n, Juruti, PA, Brazil
6 State University of Ponta Grossa, Uvaranas Campus, Av. Gal. Carlos Cavalcanti, 4748, 84030-900, Ponta Grossa, PR, Brazil
7 Engineering Faculty of the University of Porto, 4200-465, Rua Dr. Roberto Frias, s/n, Porto, Portugal
8 National University of Life and Environmental Science of Ukraine, 03041, Heroiv Oborony Str, 15, Kyiv, Ukraine
9 University of Trás-os-Montes and Alto Douro, Quinta de Prados, 5001-801, Folhadela, Vila Real, Portugal
10 Vinnytsia State Pedagogical University, 21000, Ostroz'ky Str. 32, Vinnytsia, Ukraine
11 Zhytomyr Polytechnic State University, 10005, Chudnivs'ka Str. 103, Zhytomyr, Ukraine
* Correspondence: nightwatcher2401@gmail.com (V.V.T.), ved1988mid@rambler.ru (P. I.Y.) ;
Scopus Author ID 55758299100

Received: 9.09.2023; Accepted: 28.01.2024; Published: 10.06.2024

Abstract: The possibility of algal toxin and domoic acid determination in oyster products over an undoped conducting polymer has been evaluated theoretically. Domoic acid admits various types of conducting polymer chain doping, influencing the It is shown that the galvanostatic behavior of this system becomes more dynamic than for the potentiostatic mode due to the influence of the reaction kinetics of both of the electrochemical stages on the Faraday current. Nevertheless, the undoped conducting polymer may be an optimal option for efficient domoic acid determination of domoic acid in oyster products.

Keywords: oyster; domoic acid; conducting polymers; electrochemical determination; electrochemical sensor; electrochemical oscillations; stable steady-state.

1. Introduction

Being bivalves, oysters implement an important ecological function for marine ecosystems [1–4]. They filter out great quantities of suspended material from the seawater and

produce many important nutritive substances, which is why they form an important chain in the marine food chains.

On the other hand, they consume some toxic organisms, like algae and cyanobacteria, accumulating toxins in the body [5–10], provoking oyster poisoning, one of the most frequent seafood intoxication. Depending on the symptoms, there are three to four oyster intoxication syndromes, each one caused by a concrete substance.

Due to the trophic chains, these substances come to the oyster organism and accumulate in it. Oyster consumes the toxic algae, accumulating their toxin, which thereby comes to the humans, causing intoxication (Figure 1):

Figure 1. Scheme for oyster poisoning by algal toxins.

The symptoms of oyster intoxication depend on the substance taken by the oyster and, thereby, by the human and the syndromes of amnestic, diarrheic, neurotoxic, and paralytic oyster poisoning [11–14]. The first syndrome is caused by domoic acid (Figure 2), which was used in Japan as an anthelmintic. It was first isolated from the red algae *Chondria armata*, known in the Tokunoshima Japanese dialect as *domoi*.

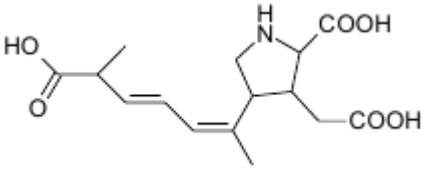

Figure 2. Domoic acid.

It may provoke ulcerogenesis, diarrhea, vomiting, and hemorrhagic gastritis first. More severe symptoms, including headache, dizziness, disorientation, loss of short-term memory, hicks, and even coma, come afterward [15–18]. In some cases, permanent short-term memory loss and peripheric neuropathy may be observed. Lethal poisoning is possible due to kidney failure in older adults, and the death incidence is in about one of every 27 intoxication cases.

For this and other reasons, the development of an efficient method capable of detecting the presence of this acid in oyster products and, thereby, preventing the intoxication is really actual [19–24], and the electrochemical methods, yet used for the detection of similar biologically active substances [25–32], could be an efficient manner to detect it.

From the domoic acid chemical composition, it is possible to conclude that it may be efficiently detected by either a cathodic or anodic process. On the other hand, considering it is a tricarbonic acid, it can be intercalated as a domoate ion towards the conducting polymer backbone [33–40]. In other words, the domoate will dope the conducting polymer, thereby yielding a composite capable of being used in a green manner for anti-worm protection of external surfaces.

Nevertheless, as domoic acid is a tricarbonic aminoacid, it may be intercalated towards the polymer matrix in three or more different manners, which may influence the double electric layer (DEL) conductivity and ionic force, leading to the instabilities, which may compromise the sensor precision and facile analytical signal interpretation.

Therefore, the development of an electrochemical sensor for domoic acid determination in oyster products and biological liquids may be difficult without an *a priori* mechanistic theoretical analysis, including the stability investigation, so this work is aimed to fulfill this need and analysis for the first time, the possibility of domoic acid electrochemical determination on an undoped conducting polymer in galvanostatic mode. This analysis will also include comparing the behavior of this system with that of similar ones [41–49].

2. Materials and Methods

As a tricarbonic aminoacid, domoic acid may be ionized in different manners, yielding three types of bipolar ions and tripolar cations and more than seven types of salts only by carboxylic groups, which reason why it perturbs the electrolyte balance in the organism. For the same reason, the doped polymer properties will become dependent on the manner by which the domoic acid enters the matrix. Either way, independently of the dopant configuration, the overall matrix domoate species will be oxidized by the Wagner reaction, yielding glycolic acid and ketoacid derivatives, the reason why the lone variable will describe the overall concentration of domoic acid forms.

Taking this into account, accepting some assumptions, and considering two types of conducting polymer doping (as the rest of them will behave analogously), we describe the galvanostatic behavior of this system as:

$$\begin{cases} \frac{da}{dt} = \frac{2}{\delta}\left(\frac{\Delta}{\delta}(a_0 - a) - r_{d1} - r_{d2}\right) \\ \frac{dp}{dt} = \frac{1}{P}(r_{d1} + r_{d2} - r_O) \\ \frac{dq}{dt} = i - i_F \end{cases} \quad (1)$$

Herein, a is the domoic acid forms overall pre-surface concentration, a_0 is their overall bulk concentration, δ is the pre-surface layer thickness, p is the doped polymer surface coverage degree, P is its maximal surface concentration, q is the anodic charge, i is the anodic current density, i_F is the Faradaic current, and the parameters r stand for the correspondent reaction rates, calculated as:

$$r_{d1} = k_{d1}(1-p)a^x \exp(-\alpha a) \exp\frac{nF\varphi_0}{RT} \quad (2)$$

$$r_{d2} = k_{d2}(1-p)a^y \exp(-\alpha a) \exp\frac{mF\varphi_0}{RT} \quad (3)$$

$$r_O = k_O p \exp\left(\frac{zF\varphi_0}{RT}\right) \quad (4)$$

Herein, the parameters k stand for the correspondent reaction rate constants, x and y are domoic acid doping reaction orders, n and m are the number of electrons transferred during the electrochemical doping, α is DEL-related parameter, describing the change of the domoate ionic form concentrations, F is the Faraday number, φ_0 is the zero-charge-related potential slope, R is the universal gas constant, and T is the absolute temperature.

The overall Faradaic current for all the electrochemical stages may be calculated as follows:

$$i_F = nFr_{d1} + mFr_{d2} + zFr_O \quad (5)$$

In galvanostatic mode, the system's behavior becomes more dynamic due to the presence of many factors influencing the anode potential change. This augments the probability of oscillatory and monotonic instabilities and makes the steady-state stability topological parameter zone. Nevertheless, this system may be efficient for domoic acid determination and domoate-doped conducting polymer synthesis, even in galvanostatic mode, as shown below.

3. Results and Discussion

To investigate the stability of the domoic acid CP-assisted determination, we analyze the equation-set (1) using linear stability theory and describe the functional Jacobian matrix as (6):

$$\begin{pmatrix} a_{11} & a_{12} & a_{13} \\ a_{21} & a_{22} & a_{23} \\ a_{31} & a_{32} & a_{33} \end{pmatrix} \quad (6)$$

In which:

$$a_{11} = \frac{2}{\delta}\left(-\frac{\Delta}{\delta} - xk_{d1}(1-p)a^{x-1}\exp(-\alpha a)\exp\frac{nF\varphi_0}{RT} + (\alpha+g)k_{d1}(1-p)a^{x}\exp(-\alpha a)\exp\frac{nF\varphi_0}{RT} - yk_{d2}(1-p)a^{y-1}\exp(-\alpha a)\exp\frac{mF\varphi_0}{RT} + (\alpha+g)k_{d2}(1-p)a^{y}\exp(-\alpha a)\exp\frac{mF\varphi_0}{RT}\right) \quad (7)$$

$$a_{12} = \frac{2}{\delta}\left(k_{d1}a^{x}\exp(-\alpha a)\exp\frac{nF\varphi_0}{RT} + k_{d2}a^{y}\exp(-\alpha a)\exp\frac{mF\varphi_0}{RT} - j\left(k_{d2}(1-p)a^{y}\exp(-\alpha a)\exp\frac{mF\varphi_0}{RT} + k_{d1}(1-p)a^{x}\exp(-\alpha a)\exp\frac{nF\varphi_0}{RT}\right)\right) \quad (8)$$

$$a_{13} = \frac{2}{\delta}\left(l\left(k_{d1}(1-p)a^{x}\exp(-\alpha a)\exp\frac{nF\varphi_0}{RT} + k_{d2}(1-p)a^{y}\exp(-\alpha a)\exp\frac{mF\varphi_0}{RT}\right)\right) \quad (9)$$

$$a_{21} = \frac{1}{P}\left(xk_{d1}(1-p)a^{x-1}\exp(-\alpha a)\exp\frac{nF\varphi_0}{RT} - (\alpha+g)k_{d1}(1-p)a^{x}\exp(-\alpha a)\exp\frac{nF\varphi_0}{RT} + yk_{d2}(1-p)a^{y-1}\exp(-\alpha a)\exp\frac{mF\varphi_0}{RT} - (\alpha+g)k_{d2}(1-p)a^{y}\exp(-\alpha a)\exp\frac{mF\varphi_0}{RT}\right) \quad (10)$$

$$a_{22} = \frac{1}{P}\left(-k_{d1}a^{x}\exp(-\alpha a)\exp\frac{nF\varphi_0}{RT} - k_{d2}a^{y}\exp(-\alpha a)\exp\frac{mF\varphi_0}{RT} + j\left(k_{d2}(1-p)a^{y}\exp(-\alpha a)\exp\frac{mF\varphi_0}{RT} + k_{d1}(1-p)a^{x}\exp(-\alpha a)\exp\frac{nF\varphi_0}{RT}\right) - k_O\exp\left(\frac{zF\varphi_0}{RT}\right) + jk_Op\exp\left(\frac{zF\varphi_0}{RT}\right)\right) \quad (11)$$

$$a_{23} = \frac{1}{P}\left(l\left(k_{d1}(1-p)a^{x}\exp(-\alpha a)\exp\frac{nF\varphi_0}{RT} + k_{d2}(1-p)a^{y}\exp(-\alpha a)\exp\frac{mF\varphi_0}{RT}\right) + k_Op\exp\left(\frac{zF\varphi_0}{RT}\right)\right) \quad (12)$$

$$a_{31} = -F\left(nxk_{d1}(1-p)a^{x-1}\exp(-\alpha a)\exp\frac{nF\varphi_0}{RT} + n(\alpha+g)k_{d1}(1-p)a^{x}\exp(-\alpha a)\exp\frac{nF\varphi_0}{RT} - myk_{d2}(1-p)a^{y-1}\exp(-\alpha a)\exp\frac{mF\varphi_0}{RT} + m(\alpha+g)k_{d2}(1-p)a^{y}\exp(-\alpha a)\exp\frac{mF\varphi_0}{RT}\right) \quad (13)$$

$$a_{32} = -F\left(-nk_{d1}a^{x}\exp(-\alpha a)\exp\frac{nF\varphi_0}{RT} - mk_{d2}a^{y}\exp(-\alpha a)\exp\frac{mF\varphi_0}{RT} + j\left(mk_{d2}(1-p)a^{y}\exp(-\alpha a)\exp\frac{mF\varphi_0}{RT} - nk_{d1}(1-p)a^{x}\exp(-\alpha a)\exp\frac{nF\varphi_0}{RT}\right) - zk_O\exp\left(\frac{zF\varphi_0}{RT}\right) + zjk_Op\exp\left(\frac{zF\varphi_0}{RT}\right)\right) \quad (14)$$

$$a_{33} = -F\left(\left(l\left(nk_{d1}(1-p)a^{x}\exp(-\alpha a)\exp\frac{nF\varphi_0}{RT} + mk_{d2}(1-p)a^{y}\exp(-\alpha a)\exp\frac{mF\varphi_0}{RT}\right) + zk_Op\exp\left(\frac{zF\varphi_0}{RT}\right)\right)\right) \quad (15)$$

Considering the unequal Faraday current impact of each of the three electrochemical stages, this system will somehow have a more dynamic behavior, even in terms of its function in galvanostatic mode.

First of all, *the oscillatory behavior* in this system is more probable than similar ones due to the positive callback, which may be caused by the DEL and surface ionic force (and related parameters) impact by both of the electrochemical stages. Another possibility of positive callback caused by DEL impacts the electrode potential and charge dynamics.

The positivity of the main diagonal elements describes this positive callback. $(\alpha+g)k_{d1}(1-p)a^{x}\exp(-\alpha a)\exp\frac{nF\varphi_0}{RT}>0$, if α>0 and or g>0, $(\alpha+g)k_{d2}(1-p)a^{y}\exp(-\alpha a)\exp\frac{mF\varphi_0}{RT}>0$, under the same conditions, $j\left(k_{d2}(1-p)a^{y}\exp(-\alpha a)\exp\frac{mF\varphi_0}{RT}+k_{d1}(1-p)a^{x}\exp(-\alpha a)\exp\frac{nF\varphi_0}{RT}+jk_{O}p\exp\left(\frac{zF\varphi_0}{RT}\right)>0\right), if\ j>0$ and $l\left(nk_{d1}(1-p)a^{x}\exp(-\alpha a)\exp\frac{nF\varphi_0}{RT}+mk_{d2}(1-p)a^{y}\exp(-\alpha a)\exp\frac{mF\varphi_0}{RT}\right)+zk_{O}p\exp\left(\frac{zF\varphi_0}{RT}\right)>0$, if l<0. This positivity is necessary for the Hopf bifurcation realization, resulting in oscillatory behavior, and these oscillations will be dependent on background electrolyte composition and monomer nature, as they directly influence the electrophysical and electrochemical properties of both DEL and polymer backbone.

In order to analyze the Jacobian determinant without cumbersome expressions, we introduce new variables and describe the determinant as (16):

$$\frac{2F}{\delta P}\begin{vmatrix}-\kappa-\Xi-\Lambda & \Sigma+T & \Phi+\Lambda\\ \Xi+\Lambda & -\Sigma-T-P & -\Phi-\Lambda-\Omega\\ -n\Xi-m\Lambda & -n\Sigma-mT-zP & -n\Phi-m\Lambda-z\Omega\end{vmatrix} \quad (16)$$

Using the determinant properties, we rearrange the matrix to (17):

$$\frac{2F}{\delta P}\begin{vmatrix}-\kappa & -P & -\Omega\\ \Xi+\Lambda & -\Sigma-T-P & -\Phi-\Lambda-\Omega\\ -n\Xi-m\Lambda & -n\Sigma-mT-zP & -n\Phi-m\Lambda-z\Omega\end{vmatrix} \quad (17)$$

And then (18):

$$\frac{2F}{\delta P}\begin{vmatrix}-\kappa & -P & -\Omega\\ \Xi+\Lambda & -\Sigma-T-P & -\Phi-\Lambda-\Omega\\ (n-m)\Lambda & -2n\Sigma-(m+n)T-(z+n)P & -2n\Phi-(m+n)\Lambda-(z+n)\Omega\end{vmatrix} \quad (18)$$

Considering that:

$$-Det\,J\begin{cases}>0, for\ steady-state\ stability\\ =0\ monotonic\ instability\end{cases} \quad (19)$$

Opening the brackets, applying the Det J<0 requisite, salient from the criterion, and changing the signs to the opposite, we rewrite the condition set as (20):

$$\kappa(2n\Sigma\Phi+\Sigma(m+n)\Lambda+\Sigma(z+n)\Omega+2nT\Phi+T(m+n)\Lambda+T(z+n)\Omega+2n\Pi\Phi+P(m+n)\Lambda+P(z+n)\Omega)>\Xi\left(2n\Omega\Sigma-(m+n)\Omega T-(z+n)\Omega P-P(2n\Phi+(m+n)\Lambda+(z+n)\Omega)\right)+\Lambda\left(2n\Omega\Sigma-(m+n)\Omega T-(z+n)\Omega P-P(2n\Phi+(m+n)\Lambda+(z+n)\Omega)-(n-m)(P\Phi+P\Lambda-\Sigma\Omega-\Sigma T)\right) \quad (20)$$

Describing a purely kinetically controlled efficient electroanalytical system, the left side of the inequity (20) generally obtains more positive values than the right side. Nevertheless, the topological zone of the steady-state stability will be limited by far more factors than in similar systems [40–49], thereby becoming far narrower. For this reason, the

use of the potentiostatic mode in amperometric measurements of this system is recommended, although the galvanostatic mode remains efficient. From the electroanalytical point of view, the steady-state stability will correspond to the linear dependence between the anode potential and domoate concentration. There are no side reactions capable of destabilizing the analyte or the polymer in the system.

The condition Det J=0 corresponds to the detection limit, manifested by the *monotonic instability*. It may be seen as an N-shaped part of the steady-state voltammogram, depicts the margin between stable and unstable states, and corresponds to steady-state multiplicity. In other words, multiple steady-states, each one unstable, coexist at this point.

In the specific case m=n=z, which is not necessarily equal to one but necessarily equal to each other, the steady-state stability becomes more efficient, and the electroanalytical signal becomes easier to interpret. Really, if we put m=n=z=N, the Jacobian determinant will be rewritten as (21):

$$\frac{2F}{\delta P}\begin{vmatrix} -\kappa-\Xi-\Lambda & \Sigma+T & \Phi+\Lambda \\ \Xi+\Lambda & -\Sigma-T-P & -\Phi-\Lambda-\Omega \\ -N\Xi-N\Lambda & -N\Sigma-NT-NP & -N\Phi-N\Lambda-N\Omega \end{vmatrix} \quad (21)$$

Using the determinant properties, we transform it into (22):

$$\frac{2F}{\delta P}\begin{vmatrix} -\kappa-\Xi-\Lambda & \Sigma+T & \Phi+\Lambda \\ \Xi+\Lambda & -\Sigma-T-P & -\Phi-\Lambda-\Omega \\ -2N\Xi-2N\Lambda & 0 & 0 \end{vmatrix} \quad (22)$$

Opening the brackets, we obtain the steady-state stability condition for the specific case of m=n=z=N as (23):

$$2N(\Xi+\Lambda)(P\Phi+P\Lambda-\Sigma\Omega-T\Omega)>0 \quad (23)$$

The process remains kinetically controlled and becomes more stable and closer to similar processes [41–49]. Analogously, the detection limit for this case will be conditioned to (24):

$$2N(\Xi+\Lambda)(P\Phi+P\Lambda-\Sigma\Omega-T\Omega)=0 \quad (24)$$

Therefore, the amperometric mode becomes more efficient in the specific case of n=m=z=N.

4. Conclusions

From the stability analysis of domoic acid determination over the undoped conducting polymer, it was possible to conclude that the galvanostatic mode becomes more dynamic than for similar systems, even in galvanostatic modes. The kinetically controlled electroanalytical system is efficient, and the analytical signal is easy to interpret and becomes even more efficient if the number of electrons transferred in all three electrochemical stages becomes equal. Nevertheless, the use of potentiostatic mode is recommended to enhance the electrochemical stability and precision of the electrochemical sensor.

Funding

This research received no external funding.

Acknowledgments

Volodymyr V. Tkach acknowledges the support of the Engineering Faculty of the University of Porto and the University of Trás-os-Montes and Alto Douro during these difficult times for Ukraine and its research.

Conflicts of Interest

The authors declare no conflict of interest.

References

1. Zhan, J.; Sun, T.; Wang, X.; Wu, H.; Yu, J. Meta-analysis reveals the species-, dose- and duration-dependent effects of cadmium toxicities in marine bivalves. *Sci. Total Environ.* **2023**, *859*, 160164, https://doi.org/10.1016/j.scitotenv.2022.160164.
2. Huang, S.; Edie, S.M.; Collins, K.S.; Crouch, N.M.A.; Roy, K.; Jablonski, D. Diversity, distribution and intrinsic extinction vulnerability of exploited marine bivalves. *Nat. Commun.* **2023**, *14*, 4639, https://doi.org/10.1038/s41467-023-40053-y.
3. Masanja, F.; Yang, K.; Xu, Y.; He, G.; Liu, X.; Xu, X.; Xiaoyan, J.; Xin, L.; Mkuye, R.; Deng, Y.; Zhao, L. Impacts of marine heat extremes on bivalves. *Front. Mar. Sci.* **2023**, *10*, 1159261, https://doi.org/10.3389/fmars.2023.1159261.
4. Maravillas, A.B.; Feliscuzo, L.S.; Estrelloso Nogra, J.A. Habitat Prediction and Knowledge Extraction for Marine Bivalves Using Machine Learning Techniques. ISMSI '23: Proceedings of the 2023 7th International Conference on Intelligent Systems, Metaheuristics & Swarm Intelligence, **2023**, 28–35, https://doi.org/10.1145/3596947.3596964.
5. Sinno-Tellier, S.; Abadie, E.; Guillotin, S.; Bossée, A.; Nicolas, M.; Delcourt, N. Human shellfish poisoning: Implementation of a national surveillance program in France. *Front. Mar. Sci.* **2022**, *9*, 1089585, https://doi.org/10.3389/fmars.2022.1089585.
6. Ayache, N.; Bill, B.D.; Brosnahan, M.L.; Campbell, L.; Deeds, J.R.; Fiorendino, J.M.; Gobler, C.J.; Handy, S.M.; Harrington, N.; Kulis, D.M.; McCarron, P.; Miles, C.O.; Moore, S.K.; Nagai, S.; Trainer, V.L.; Wolny, J.L.; Young, C.S.; Smith, J.L. A survey of *Dinophysis* spp. and their potential to cause diarrhetic shellfish poisoning in coastal waters of the United States. *J. Phycol.* **2023**, *59*, 658–680, https://doi.org/10.1111/jpy.13331.
7. Wang, X.; Bouzembrak, Y.; Marvin, H.J.P.; Clarke, D.; Butler, F. Bayesian Networks modeling of diarrhetic shellfish poisoning in *Mytilus edulis* harvested in Bantry Bay, Ireland. *Harmful Algae*. **2022**, *112*, 102171, https://doi.org/10.1016/j.hal.2021.102171.
8. Tebben, J.; Zurhelle, C.; Tubaro, A.; Samdal, I.A.; Krock, B.; Kilcoyne, J.; Sosa, S.; Trainer, V.L.; Deeds, J.R.; Tillmann, U. Structure and toxicity of AZA-59, an azaspiracid shellfish poisoning toxin produced by *Azadinium poporum* (Dinophyceae). *Harmful Algae* **2023**, *124*, 102388, https://doi.org/10.1016/j.hal.2023.102388.
9. Cadaillon, A.M.; Almandoz, G.O.; Hernando, M.P.; Saravia, L.; Maldonado, S.; Schloss, I.R. Spatiotemporal distribution of paralytic shellfish poisoning (PSP) toxins in Beagle Channel (South America) during 2005–2017. *Progr. Oceanography.* **2022**, *204*, 102757, https://doi.org/10.1016/j.pocean.2022.102757.
10. Straquadine, N.R.W.; Kudela, R.M.; Gobler, C.J. Hepatotoxic shellfish poisoning: Accumulation of microcystins in Eastern oysters (*Crassostrea virginica*) and Asian clams (*Corbicula fluminea*) exposed to wild and cultured populations of the harmful cyanobacteria, *Microcystis*. *Harmful Algae* **2022**, *115*, 102236, https://doi.org/10.1016/j.hal.2022.102236.
11. Petroff Rebekah, L.; Williams, C.; Li, J.-L.; MacDonald James, W.; Bammler Theo, K.; Richards, T.; English Christopher, N.; Baldessari, A.; Shum, S.; Jing, J.; Isoherranen, N.; Crouthamel, B.; McKain, N.; Grant Kimberly, S.; Burbacher Thomas, M.; Harry, G.J. Prolonged, Low-Level Exposure to the Marine Toxin, Domoic Acid, and Measures of Neurotoxicity in Nonhuman Primates. *Environ. Health Perspect.* **2022**, *130*, 097003, https://doi.org/10.1289/EHP10923.
12. Ji, Y.; Yan, G.; Wang, G.; Liu, J.; Tang, Z.; Yan, Y.; Qiu, J.; Zhang, L.; Pan, W.; Fu, Y.; Li, T.; Luo, X.; Lan, W.; Wang, Z.; Li, W.; Li, A. Prevalence and distribution of domoic acid and cyclic imines in bivalve mollusks from Beibu Gulf, China. *J. Hazard. Mater.* **2022**, *423*, 127078, https://doi.org/10.1016/j.jhazmat.2021.127078.
13. Moreno, A.R.; Anderson, C.; Kudela, R.M.; Sutula, M.; Edwards, C.; Bianchi, D. Development, calibration, and evaluation of a model of Pseudo-nitzschia and domoic acid production for regional ocean modeling studies. *Harmful Algae* **2022**, *118*, 102296, https://doi.org/10.1016/j.hal.2022.102296.

14. Zheng, G.; Wu, H.; Che, H.; Li, X.; Zhang, Z.; Peng, J.; Guo, M.; Tan, Z. Residue Analysis and Assessment of the Risk of Dietary Exposure to Domoic Acid in Shellfish from the Coastal Areas of China. *Toxins* **2022**, *14*, 862, https://doi.org/10.3390/toxins14120862.
15. Anderson, M.; Valera, M.; Schnetzer, A. Co-occurrence of freshwater and marine phycotoxins: A record of microcystins and domoic acid in Bogue Sound, North Carolina (2015 to 2020). *Harmful Algae* **2023**, *125*, 102412, https://doi.org/10.1016/j.hal.2023.102412.
16. Nishizawa, S.; Ouchi, H.; Suzuki, H.; Ohnishi, T.; Sasaki, S.; Oyagi, Y.; Kanakogi, M.; Matsumura, Y.; Nakagawa, S.; Asakawa, T.; Egi, M.; Inai, M.; Yoshimura, F.; Takita, R.; Kan, T. Total synthesis of (−)-domoic acid, a potent ionotropic glutamate receptor agonist and the key compound in oceanic harmful algal blooms. *Org. Biomol. Chem.* **2023**, *21*, 1653–1656, https://doi.org/10.1039/d2ob02325C.
17. Du, M.; Jin, Y.; Fan, J.; Zan, S.; Gu, C.; Wang, J. A new pathway for anaerobic biotransformation of marine toxin domoic acid. *Environ. Sci. Pollut. Res.* **2023**, *30*, 5150–5160, https://doi.org/10.1007/s11356-022-22368-3.
18. Li, Z.; Wang, J.; Fan, J.; Yue, H.; Zhang, X. Marine toxin domoic acid alters protistan community structure and assembly process in sediments. *Mar. Environ. Res.* **2023**, *191*, 106131, https://doi.org/10.1016/j.marenvres.2023.106131.
19. Wang, Q.F.; Liang, L.J.; Sun, J.B.; Zhou, J. Application of a reversed-phase ionic liquid dispersive liquid-liquid microextraction method for the extraction and preconcentration of domoic acid from urine samples. *Heliyon* **2022**, *8*, e10152, https://doi.org/10.1016/j.heliyon.2022.e10152.
20. Juneja, S.; Zhang, B.; Nujhat, N.; Wang, A.X. Quantitive Sensing for Domoic Acid from Shellfish Using Biological Photonic Crystal Enhanced SERS Substrates. *Molecules* **2022**, *27*, 8364, https://doi.org/10.3390/molecules27238364.
21. Zhao, L.; Guo, H.; Chen, H.; Zou, B.; Yang, C.; Zhang, X.; Gao, Y.; Sun, M.; Wang, L. A Rapid and Sensitive Aptamer-Based Biosensor for Amnesic Shellfish Toxin Domoic Acid. *Bioengineering* **2022**, *9*, 684, https://doi.org/10.3390/bioengineering9110684.
22. Yang, A.; Zhang, H.; Yang, Y.; Jiang, Z. Progresses of the Influencing Factors and Detection Methods of Domoic Acid. *Processes* **2023**, *11*, 592, https://doi.org/10.3390/pr11020592.
23. Hendrickson, O.D.; Zvereva, E.A.; Solopova, O.N.; Zherdev, A.V.; Sveshnikov, P.G.; Eremin, S.A.; Dzantiev, B.B. Double Immunochromatographic Test System for Sensitive Detection of Phycotoxins Domoic Acid and Okadaic Acid in Seawater and Seafood. *Micromachines* **2022**, *13*, 1506, https://doi.org/10.3390/mi13091506.
24. Wang, L.; Wen, L.; Chen, Y.; Wang, F.; Li, C. Construction of ratiometric fluorescence sensor and test strip with smartphone based on molecularly imprinted dual-emission quantum dots for the selective and sensitive detection of domoic acid. *Chemosphere* **2022**, *304*, 135405, https://doi.org/10.1016/j.chemosphere.2022.135405.
25. Bahadori, Y.; Razmi, H. Design of an electrochemical platform for the determination of diclofenac sodium utilizing a graphenized pencil graphite electrode modified with a Cu–Al layered double hydroxide/chicken feet yellow membrane. *New J. Chem.* **2021**, *45*, 14616–14625, https://doi.org/10.1039/d1nj02258j.
26. Parrilla, M.; Slosse, A.; Van Echelpoel, R.; Montiel, N.F.; Van Durme, F.; De Wael, K. Portable Electrochemical Detection of Illicit Drugs in Smuggled Samples: Towards More Secure Borders. *Chem. Proc.* **2021**, *5*, 44, https://doi.org/10.3390/CSAC2021-10612.
27. Santra, S.; Sarkar, B.R.; Doloi, B.; Bhattacharyya, B. Investigation through novel tool-electrode feeding approach on electrochemical discharge machining of glass. *Proc. Inst. Mech. Eng. B J. Eng. Manuf.* **2023**, *237*, 1207-1219, https://doi.org/10.1177/0954405422211234769.
28. de Carvalho, R.C.; Betts, A.J.; Cassidy, J.F. Diclofenac determination using CeO_2 nanoparticle modified screen-printed electrodes – A study of background correction. *Microchem. J.* **2020**, *158*, 105258, https://doi.org/10.1016/j.microc.2020.105258.
29. Fadhel, S.; Al-Kadumi, A.S.H.; Imran, N.A.; Abdulateef, M.H. A Developed Method for the Estimation of Diclofenac Sodium via Coupling with Diazotized 4-Aminoacetophenone. *Egypt J. Chem.* **2021**, *64*, 3703–3709, https://doi.org/10.21608/ejchem.2021.68509.3497.
30. Li, Y.; Wu, X.; Wu, Z.; Zhong, M.; Su, X.; Ye, Y.; Liu, Y.; Tan, L.; Liang, Y. Colorimetric sensor array based on CoOOH nanoflakes for rapid discrimination of antioxidants in food. *Anal. Methods* **2022**, *14*, 2754–2760, https://doi.org/10.1039/D2AY00692H.

31. Garima; Sachdev, A.; Matai, I. An electrochemical sensor based on cobalt oxyhydroxide nanoflakes/reduced graphene oxide nanocomposite for detection of illicit drug-clonazepam. *J. Electroanal. Chem.* **2022**, *919*, 116537, https://doi.org/10.1016/j.jelechem.2022.116537.
32. Ramanavicius, S.; Ramanavicius, A. Conducting Polymers in the Design of Biosensors and Biofuel Cells. *Polymers* **2021**, *13*, 49, https://doi.org/10.3390/polym13010049.
33. Ramanaviciene, A.; Plikusiene, I. Polymers in Sensor and Biosensor Design. *Polymers* **2021**, *13*, 917, https://doi.org/10.3390/polym13060917.
34. Mekgoe, N.; Mabuba, N.; Pillay, K. Graphic Carbon Nitride-Silver Polyvinylpyrrolidone Nanocomposite Modified on a Glassy Carbon Electrode for Detection of Paracetamol. *Front. Sens.* **2022**, *3*, 827954, https://doi.org/10.3389/fsens.2022.827954.
35. Thadathil, A.; Pradeep, H.; Joshy, D.; Ismail, Y.A.; Periyat, P. Polyindole and polypyrrole as a sustainable platform for environmental remediation and sensor applications. *Mater. Adv.* **2022**, *3*, 2990–3022, https://doi.org/10.1039/D2MA00022A.
36. Alberti, G.; Zanoni, C.; Losi, V.; Magnaghi, L.R.; Biesuz, R. Current Trends in Polymer Based Sensors. *Chemosensors* **2021**, *9*, 108, https://doi.org/10.3390/chemosensors9050108.
37. Namsheer, K.; Rout, C.S. Conducting polymers: a comprehensive review on recent advances in synthesis, properties and applications. *RSC Adv.* **2021**, *11*, 5659–5697, https://doi.org/10.1039/D0RA07800J.
38. Glosz, K.; Stolarczyk, A.; Jarosz, T. Electropolymerised Polypyrroles As Active Layers for Molecularly Imprinted Sensors: Fabrication and Application. *Materials* **2021**, *14*, 1369, https://doi.org/10.3390/ma14061369.
39. Bagheri, A.; Hassani Marand, M. Voltammetric and Potentiometric Determination of Cu^{2+} Using an Overoxidized Polypyrrole Based Electrochemical Sensor. *Russ. J. Electrochem.* **2020**, *56*, 453–461, https://doi.org/10.1134/S1023193520060026.
40. Joshi, N.C.; Malik, S.; Gururani, P. Utilization of Polypyrrole/ZnO Nanocomposite in the Adsorptive Removal of Cu^{2+}, $Pb^{2+}$and Cd $^{2+}$ Ions from Wastewater. *Lett. Appl. NanoBioSci.* **2021**, *10*, 2339–2351, https://doi.org/10.33263/LIANBS103.23392351.
41. Das, I.; Goel, N.; Agrawal, N.R.; Gupta, S.K. Growth Patterns of Dendrimers and Electric Potential Oscillations during Electropolymerization of Pyrrole using Mono- and Mixed Surfactants. *J. Phys. Chem. B* **2010**, *114*, 12888-12896, https://doi.org/10.1021/jp105183q.
42. Das, I.; Goel, N.; Gupta, S.K.; Agrawal, N.R. Electropolymerization of pyrrole: Dendrimers, nano-sized patterns and oscillations in potential in presence of aromatic and aliphatic surfactants. *J. Electroanal. Chem.* **2012**, *670*, 1-10, https://doi.org/10.1016/j.jelechem.2012.01.023.
43. Aoki, K.; Mukoyama, I.; Chen, J. Competition between Polymerization and Dissolution of Poly(3-methylthiophene) Films. *Russ. J. Electrochem.* **2004**, *40*, 280-285, https://doi.org/10.1023/B:RUEL.0000019665.59805.4c.
44. Tkach, V.; Kushnir, M.; Romaniv, L.; de Oliveira, S.; Ivanushko, Y.; Nazymok, Y.; Ahafonova, O.; Yagodynets, P.; Olimpio, A.; Derevianko, N.; Zavhorodniy, M.; Odyntsova, V.; Krasko, M.; Vasylieva, O.; Hrabovska, O.; Musayeva, D.; Sharipova, R.; Samadov, B.; Niyazov, L.; Kushnir, L. The Theoretical Description for Ibotenic Acid and Muscimol Electrochemical Determination in Mushroom Pulp and Mushroom-based Alcoholic Beverages on Nano- CuS Composite with Conducting Polymer. *Lett. Appl. NanoBioSci.* **2024**, *13*, 37, https://doi.org/10.33263/LIANBS131.037.
45. Tkach, V.; Kucher, M.; Kushnir, M.; Ivanushko, Y.; Akinay, Y.; Karakoyun, N.; Yagodynets, P.; Kormosh, Z. The Theoretical Description for Psilocin Electrochemical Determination over Cobalt Oxyhydroxide Graphical abstract. *Orbital Elec. J. Chem.* **2023**, *15*, 27–30, http://dx.doi.org/10.17807/orbital.v15i1.18012.
46. Tkach, V.; Kushnir, M.; de Oliveira, S.; Ivanushko, Y.; Tkach, V.; Mytrofanova, H.; Zadoia, A.; Yagodynets, P.; Kormosh, Z.; Luganska, O.; Pochenchuk, G. Theoretical Description for Copper (II) Electrochemical Determination and Retention on a 1(2-pyridilazo)-2- naphthole-Modified Anode. *Lett. Appl. NanoBioSci.* **2021**, *10*, 2078–2084, https://doi.org/10.33263/LIANBS102.20782084.
47. Tkach, V.; Kushnir, M.; Ivanushko, Y.; Молодяну, А.; Mytchenok, M.; Ahafonova, O.; de Oliveira, S.; Yagodynets, P.; Kormosh, Z.; Bredikhina, Y.; Luganska, O. Theoretical Description for the Galvanostatic Electrode Pretreatment, Yielding Thiourea-Based Active Surface for Cathodic Conducting Polymer Deposition. *Lett. Appl. NanoBioSci.* **2020**, *9*, 1333–1338, http://dx.doi.org/10.33263/LIANBS93.13331338.
48. Tkach, V.V.T.; Kushnir, M.V.; de Oliveira, S.C.; G. Ivanushko, Y.; B. Sykyrytska, T.; G. Biryuk, I.; V. Luganska, O.; V. Kopiika, V.; I. Yagodynets´, P.; O. Kormosh, Z.; V. Morozova, T.; I. F. Martins, J.; Vaz dos Reis, L. Descripción teórica de la detección electroquímica del fármaco pilocarpina, asistida por el compuesto de colorante escuárico con el oxihidróxido de vanadio (III). *Rev. Colomb. Cien. Quím.* **2023**, *52*, https://doi.org/10.15446/rcciquifa.v52n1.109398.

49. Tkach, V.; Kushnir, M.; de Oliveira, S.; Ivanushko, Y.; Nazymok, Y.; Olimpio, A.; Luganska, O.; Yeshchenko, Y.; Omelianchyk, L.; Gencheva, V.; Kopiika, V.; Yagodynets´, P.; Kormosh, Z.; Palytsia, Y. THE THEORETICAL EVALUATION OF THE POSSIBILITY OF THE COO(OH)-ASSISTED PARAQUAT ELECTROCHEMICAL DETECTION. *Appl. J. Environ. Eng. Sci.* **2023**, *9*, 9-12, https://doi.org/10.48422/IMIST.PRSM/ajees-v9i2.33282.